Propellants, Explosives, Pyrotechnics

WILEY-VCH

Propellants, Explosives, Pyrotechnics

RESEARCH ARTICLE OPEN ACCESS

Processing, Characterization, and Detonation Testing of Explosive/Wax/Graphite Charges With CL-20/HMX Cocrystals

Michael Herrmann[1] | Peter Gerber[1] | Tobias Baust[2]

[1]Department Energetic Materials, Fraunhofer Institut für Chemische Technologie ICT, Pfinztal, Germany | [2]TDW Gesellschaft für verteidigungstechnische Wirksysteme mbH, Schrobenhausen, Germany

Correspondence: Michael Herrmann (michael7herrmann@gmail.com)

Keywords: CL-20/HMX cocrystal | processing | microstructure | small-scale detonation test

ABSTRACT

Granulates of explosive/wax/graphite formulations, oktogen/wax/graphite formulation (OWC), hexogen/wax/graphite formulation (HWC), PBX-formulation of the FhG ICT (PHX) 151, and PHX 153 with 1,3,5,7-tetranitro-1,3,5,7-tetrazocane (HMX), 1,3,5-trinitro-1,3,5-triazinan (RDX), and 2,4,6,8,10,12-hexanitrohexaazaisowurtzitane/HMX (CL-20/HMX) cocrystal were produced by dissolving wax with petroleum benzine, blending and kneading ingredients, and evaporation of solvent or granulates were commercially obtained. The mixtures were pressed into cylinders, and the microstructure and performance of the pressed forms were investigated by means of X-ray diffraction and small-scale detonation tests. The granulates consist of 94.5% explosive, 4.5% wax, and 1% graphite. The investigations show different mechanical strengths of embedded explosive crystals, with higher mechanical stability of RDX and cocrystal compared to HMX. Moreover, the cocrystal formulation PHX 153 was less sensitive to friction and impact than the OWC, particularly the friction force increased to 324 N. The small-scale detonation tests yielded 8.91 km/s and 28.3 GPa detonation velocity and pressure of the cocrystal-based PHX 153, and thus a significantly increased detonation performance by 0.31 km/s (3.6%) and 1.7 GPa (6.4%) compared to the HMX-based OWC. Hence, the CL-20/HMX cocrystal is a promising candidate to increase the detonation performance, for example, of pressed explosive formulations.

1 | Introduction

Crystal engineering by cocrystallization is a promising approach to improving energetic materials by composing two or more already well-known or even established components. Its application yields new structural models with defined molar ratios and extends the property spectra of energetic fillers, for example, for application in plastic-bonded explosives (PBX). In recent years, many papers have been published combining, for example, 2,4,6,8,10,12-hexanitrohexaazaisowurtzitane (CL-20) with 2,7,6-trinitrotoluol, 1,3,5,7-tetranitro-1,3,5,7-tetrazocane (HMX), or 1,3,5-trinitro-1,3,5-triazinan (RDX) [1–3]. Herein, the CL-20/HMX cocrystal has been promoted as a promising candidate for explosives applications, combining the high detonation performance of CL-20 with the lower sensitivity of HMX [2]. Whereas many cocrystal systems were characterized on a theoretical to laboratory scale basis, few papers report feasibility tests and performance characterization on a technical scale, including formulation work and detonation testing. At the Fraunhofer Institute for Chemical Technology (ICT), research on the

Abbreviations: BAM, Bundesamt für Materialforschung; CJ, Chapman-Jouguet; CL-20, 2,4,6,8,10,12-hexanitrohexaazaisowurtzitane; CoD, coefficients of determination; DAX, disc acceleration experiment; EOS, equation of state; FhG, Fraunhofer Gesellschaft/Society; HMX, 1,3,5,7-tetranitro-1,3,5,7-tetrazocane; HWC, hexogen/wax/graphite formulation; ICT, Fraunhofer Institute for Chemical Technology, Pfinztal, Germany; OWC, oktogen/wax/graphite formulation; PBX, plastic-bonded explosives; PDV, photonic Doppler velocimetry; PHX, PBX-formulation of the FhG ICT; RDX, 1,3,5-trinitro-1,3,5-triazinan; VOD, velocity of detonation; XRD, X-ray diffraction..

TABLE 1 | Compositions of the formulations plastic-bonded explosives (PBX)-formulation of the FhG ICT (PHX) 151 and PHX 153.

PHX 151	Mass fraction [%]	PHX 153	Mass fraction [%]
HMX Grade B Class 3	63	Coarse HMX/CL-20	65.85
HMX Grade B Class 5	31.5	Milled HMX/CL-20	28.65
Graphite	1.0	Graphite	1.0
Paraffin	4.5	Paraffin	4.5

preparation and feasibility of CL-20/HMX cocrystal charges has been carried out, including synthesis, up-scaling, and modification of crystal qualities [4–7]. The investigations revealed high-quality co-crystals, still high impact sensitivities (1.5–4.5 Nm) but comparably low friction sensitivities (120–192 N). In this work, we present further investigations to evaluate the detonation performance capability and processability of the cocrystal, which include technical scale explosive granulation, pellet production, microstructure characterization, and small-scale detonation testing.

2 | Experimental

2.1 | Granulate and Pellets Production

The formulation was laid out to match 150 g final product for each granulate with mass fractions of 94.5% energetic filler, 4.5% paraffin wax (Merck), and 1% graphite. The energetic filler was composed of 2/3 coarse material and 1/3 fine material by mass, with median particle size and span values of the cocrystal fractions of 157 µm and 1.48 and 18.56 µm and 1.97, respectively. The wax with a melting point of 57–60°C was dissolved in petroleum benzine overnight at 40–60°C. The binder, graphite, and the energetic filler were mixed in a horizontal kneader from the company IKA, and the solvent was evaporated under slow heating until the wax wetted the energetic filler homogenously. Granulates of two explosive formulations were produced, PBX-formulation of the FhG ICT (PHX) 151 with commercial HMX grades and PHX 153 with CL-20/HMX cocrystal produced at the Fraunhofer ICT by batch reaction cocrystallization [8]. Details of the composition can be seen in Table 1.

Besides the ICT products, two commercial granulates, hexogen/wax/graphite formulation (HWC) and OWC, based on RDX and HMX, were used as reference materials with the same overall mass ratios. A commercial comparable formulation based on CL-20 is not available, and the values of the impact and friction sensitivity of such a formulation are so low that it was not possible to press this formulation to achieve pellets without a case. OWC and HWC were purchased from Chemring Nobel AS, Sætre, Norway, with the specifications HMX; Octogen desensitized, OWC (94.5/4.5/1), lot number DDP21E0025-0003, and RDX; Hexogen desensitized, HWC (94.5/4.5/1), lot number DDP21K0192-0002. Both Formulation consists of 94.5 mass percent of energetic filler, 4.5 mass percent wax, and 1% of graphite. These materials are proposed for shaped, blast, and fragmentation, and booster charges as typical applications.

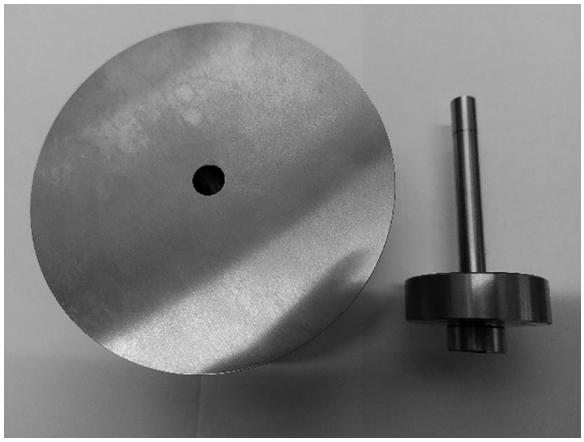

FIGURE 1 | Pressing tool for explosive pellets.

A new pressing tool, model 20 S from the Paul-Otto Weber GmbH [9], was purchased to produce testing forms. Press die, ram, and plunger of the tool are manufactured from high-alloy, hardened tool steel with optically polished die surfaces, which enables to formation of stable, plane-parallel, homogeneous, and compact forms (Figure 1). The granulates were pressed in a laboratory press (PWV 6 ES-Servo also from Paul-Otto Weber GmbH) to 10–15 cylinders of each formulation with 10 mm diameter and 10 mm height—hereinafter referred to as pellets. The forming pressure was 0.1 GPa, which corresponds to an 8–10 kN pressing force. A pressure of 0.1 GPa is very reasonable. If the forming pressure is too low, the achieved density of the pellets is too low. At higher pressures, the crystals break during the pressing process. Table 2 provides an overview of formulations and sources.

2.2 | Sensitivity Testing

Mechanical sensitivities of the granulates of the PHX formulations were measured by means of Bundesamt für Materialforschung (BAM) fall hammer and friction tests to determine the limiting impact energy and friction force.

2.3 | Micro and Crystal Structure Characterization (X-ray Diffraction)

X-ray diffraction (XRD) patterns of a fine cocrystal sample obtained by batch reaction cocrystallization [4], the granulates and the pressed pellets were measured with a Bragg-Brentano

TABLE 2 | Overview of formulations, samples, and sources.

Formulation	Description	Form	Source
OWC	HMX/wax/graphite	Granulate & pellets	Chemring Nobel As
HWC	RDX/wax/graphite	Granulate & pellets	commercial
PHX 151	HMX/wax/graphite	Granulate & pellets	FhG ICT product
PHX 153	cocrystal/wax/graphite	Granulate & pellets	FhG ICT product

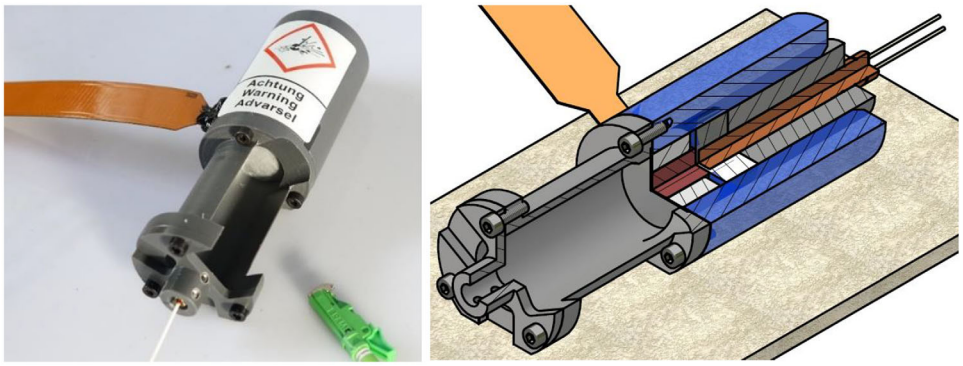

FIGURE 2 | Testing device for a simultaneous measurement of detonation velocity and pressure in small-scale detonation tests.

diffractometer, D8 Advance from Bruker AXS, equipped with copper tube, nickel Kβ-filter, two Soller collimators (2.5°), variable divergence slit (V6), and silicon-strip detector (LynxEye with 3 °2θ detector opening). Patterns were measured between 10 and 50 °2θ with 0.01 °2θ step width and 20 s counting time per step.

2.4 | Small-scale Detonation Test

The pellets were experimentally characterized by means of a small-scale detonation measurement combined with a disc acceleration experiment (DAX). The DAX was adapted from literature [10] and developed further at the Fraunhofer ICT to be able to apply it to very small explosive samples. In addition, to measure the velocity of detonation (VOD), a small-scale detonation-velocity measurement test setup, developed at the Fraunhofer ICT [11], was integrated. For instance, Figure 2 depicts a detonation tool and a related schematic drawing. Herein, the explosive charge is in the upper cylindrical structure, and a short-circuit-pin-array in the form of a flex board is inserted laterally for measuring the detonation velocity on the outside of the charge within a 6 mm distance. Initiation takes place via a detonator, which first acts on a poly(methyl methacrylate) gap to slightly attenuate and broaden the shock wave prior to initiating the sample charge. The ignition chain was evaluated in simulations to ensure a well-defined and preferably flat shock wave. Although a standard detonator (Dynawell U, no 8) was used, its performance characteristics are very well known due to prior works using photon-doppler-velocimetry (PDV) to measure the velocity of the capsule bottom to validate the simulation model of the detonator used to design the ignition chain here. The detonation wave running through the main charge is then recorded by the short circuit pin-array. Two samples (10 mm diameter, 5 mm height) were stacked to define the main charge. Although the shock wave to initiate the main charge was relatively homogeneous, a run distance of the first 4 mm was excluded in the VOD measurement to ensure a detonation wave with a steady curvature. This is essential when measuring the detonation velocity at the outside of a cylindrical charge. In previous works, a steady measurement on HNS-pellets (5 mm length, used in exploding foil initiators) on only two millimeters has been proven to be statistically reliable [11]. Finally, the detonation wave accelerates an aluminum disc (flyer), being recorded by a PDV probe facing the flyer, which is then used in impedance matching to determine the detonation pressure. The flyer consists of annealed 99.0% aluminum with 0.5 mm thickness and forms the interface to a measurement technology, where a PDV-probe is mounted in the lower part of the structure, 50 mm from the aluminum disc. For our experiments, flex boards with 12 effectively used short-circuit contacts were manufactured using two 8-channel scopes with a bandwidth of 1 GHz. The heterodyne PDV system utilizes a 1550 nm infrared laser, whereby the Doppler shift is recorded with a 16 GHz scope at 40 GS/s. Furthermore, a curvature correction of the detonation velocity was carried out via the axially defined distance between the probe locations and the assumed initiation point, although the impact of the correction was small due to the previously described measures. Further details of the small-scale detonation test are reported elsewhere [12].

3 | Results

3.1 | Granulate and Pellets Production

Figure 3 depicts the CL-20/HMX granulate PHX 153 (left) and the sample portfolio used for micro- and crystal structure investigations, including a pressed pellet and a small quantity of granulate of each formulation (right). The pressing yielded compact stable

FIGURE 3 | Granulate of the cocrystal formulations PBX-formulation of the FhG ICT (PHX) 153 (left) and granulate samples and pressed pellets used for the microstructure characterization (right).

cylinders of the formulations OWC, HWC, and PHX 153, but less stable PHX 151 pellets.

As densities of the pressed explosive formulations are required to determine the detonation pressures from the PDV data, sample volumes and weights of 10 cylinders per formulation (only the main charges, not the booster charges) were determined with a sliding caliper and a high-resolution balance. The measurements yielded mean densities of 1.669 ± 0.007 g/cm^3 for HWC, 1.763 ± 0.005 g/cm^3 for OWC, and 1.790 ± 0.002 g/cm^3 for PHX 153.

3.2 | Sensitivity Testing

The BAM sensitivity testing of the granulates yielded 5 Nm limiting impact energy and 160 N limiting friction force of HMX-based PHX 151 and 6 Nm and 324 N of cocrystal-based PHX 153. Thus, according to United Nations recommendations, sensitivity values of both granulates fall in the ranges 4–35 Nm and 80–350 N for sensitive materials, but the cocrystal-based PHX 153 revealed a slightly lower sensitivity against impact and a significantly lower sensitivity against friction compared to PHX 151.

3.3 | Micro- and Crystal Structure of Granulates and Pellets (XRD)

A diffraction pattern section of the raw cocrystal sample and its evaluation by means of Rietveld refinement [13] is presented in Figure 4. During the evaluation procedure, a theoretical diffraction pattern was calculated starting with literature data [2], and the calculated (red) pattern was fit to the measured pattern (black) with a non-linear least squares fitting system provided by the program TOPAS from Bruker AXS [14]. The fit identifies the co-crystal structure unambiguously and shows that no extra peaks, e.g., of HMX and CL-20, emerged from the background, which means no crystalline impurities or unconverted precursors were found in the co-crystallized product. Moreover, the fit with the monoclinic space group P 1 2_1/c 1 yielded refined lattice parameters a = 16.508 Å, b = 10.007 Å, c = 12.248 Å, $\beta = 100.0°$, a cell volume of 1992.4 Å^3, and a calculated density of 1.954 g/cm^3 – a little bit higher than the reported value of 1.945 g/cm^3 at room temperature. Furthermore, the plot shows differences in peak intensities, which most likely represent a preferred orientation on (200), which was also refined during the evaluation. However, with still significant intensity differences, the weighted pattern error of the fit (R_{wp}) was acceptable at 10.7.

The analysis of the granulates and pellets of HWC, OWC, PHX 151, and PHX 153 yielded the expected crystal structures of RDX, β-HMX, and the CL-20/HMX co-crystal. Furthermore, HMX impurities were found in the RDX-based HWC, and peaks of crystalline wax (n-paraffin) and graphite in both granulates and pellets. For instance, Figure 5 depicts the patterns of HWC, PHX 151, and PHX 153 granulates with reference position bars from the International Centre for Diffraction Data [15] and our co-crystal measurement (Figure 4). Ragged peak profiles in the diffraction patterns of the granulates, versus rather smooth profiles in the pellets, indicate that large coherent crystal domains in the granulates were comminuted during the pressing process. No proper Rietveld analysis was possible with the ragged profiles. Hence, symmetrical pseudo-Voigt functions were fitted to the diffraction profiles, and cumulative peak width distributions (Figure 6) were evaluated using a sigmoidal fit $y = 1 - 1/[x/x_0]^p$ (logistic fit of the program OriginPro), where x_0 and p are the distribution center and power.

The results of the peak profile analyses are compiled in Table 3 together with parameters of the Rietveld analysis, and the median peak widths of the granulates and pellets (distribution centers) are compared to each other in Figure 7.

The Rietveld analysis yielded relatively low crystal sizes (not calibrated) of 60 and 69 nm for the HMX-based OWC and PHX 151 pellets compared to 89 and 111 nm of the RDX- and CL-20/HMX-based pellets. Furthermore, the statistical peak profile analysis revealed significant peak broadening, where after pressing the median peak widths increased from 0.063 and 0.065 °2θ to 0.114 and 0.116 °2θ in case of PHX 153 and HWC, and even from 0.077 and 0.087 °2θ to 0.168 and 0.176 °2θ in case of the HMX-based formulations PHX 151 and OWC, respectively. So far, the XRD investigations showed that domains of embedded crystals were comminuted during the pressing of the granulates to pellets and revealed higher mechanical strengths of RDX crystals and the CL-20/HMX cocrystals compared to HMX crystals.

3.4 | Small-scale Detonation Test

The detonation velocities were determined using a linear regression between probe distance and the signal time at which the

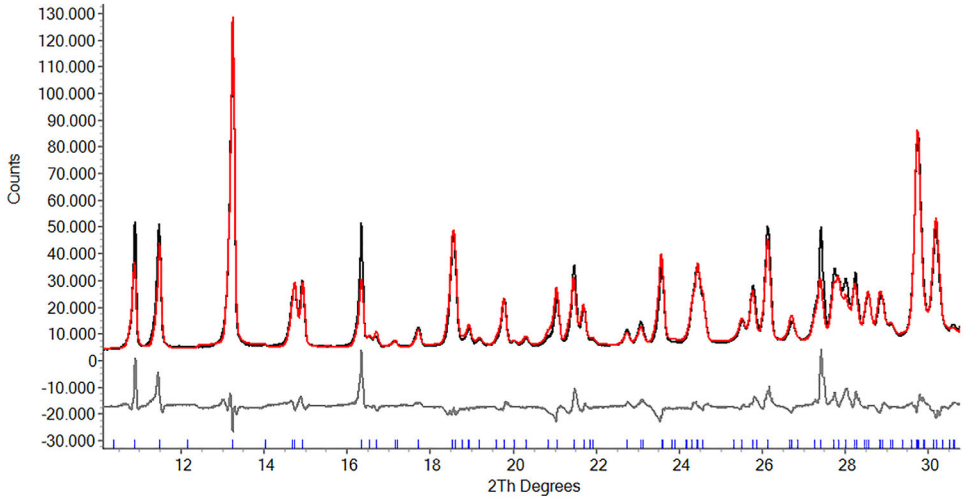

FIGURE 4 | Section of a Rietveld plot of the raw cocrystal sample. Measured pattern (black), fitted pattern (red), differences (grey), and peak position markers (blue).

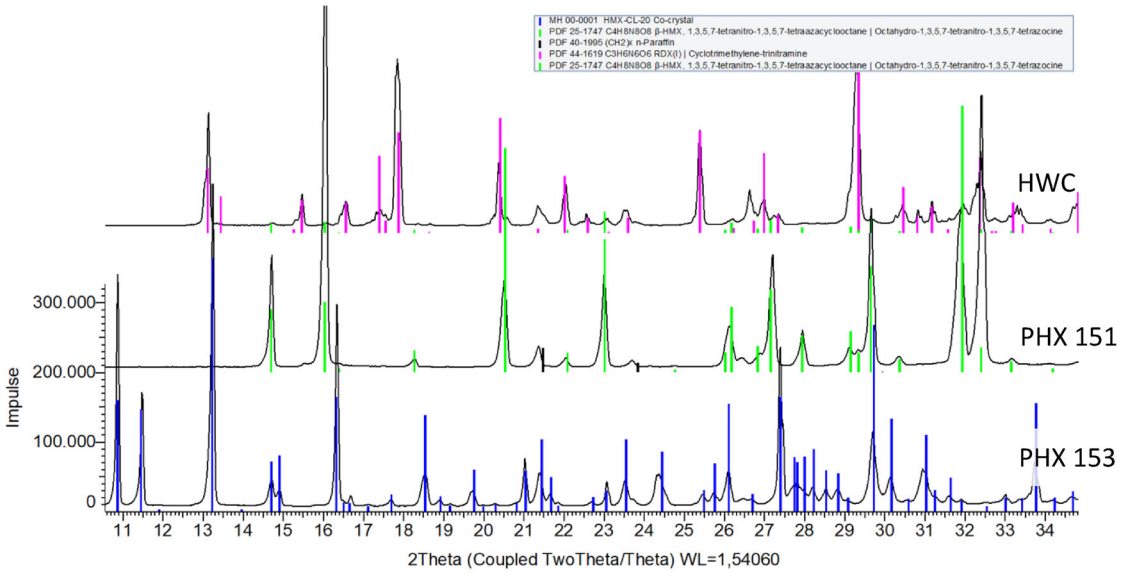

FIGURE 5 | Sections of diffraction patterns of the granulates hexogen/wax/graphite formulation (HWC) (top), PHX 151 (middle), and PBX-formulation of the FhG ICT (PHX) 153 (bottom), and identification of the crystalline phases β-HMX (PDF 25-1747, green bars), RDX (PDF 44-1619, magenta bars), CL-20/HMX-co-crystal (own reference, blue bars), and n-paraffin (PDF 40-1995, black bars).

detonation front short-circuits the contacts. The pin positions were already projected onto the corresponding axial positions according to the curvature correction. The nominal pin spacing within the flex board was 0.6 mm, and the total real measuring distance was therefore 6.6 mm. Due to the short start-up distance, the influence of the curvature correction is approximately 5% of the detonation velocity, so that the absolute values are subject to a low degree of uncertainty. However, this is not relevant for the relative comparison of the explosives, as the geometric conditions are identical for all explosives. For instance, the linear regression between probe distances and the signal time at which the detonation front short-circuits the contacts is shown in Figure 8 in the case of a cocrystal-based PHX 153 pellet. The slope of the regression yielded a detonation velocity of 8.92 mm/µs for that sample. The given error results from the uncertainty of the linear regression.

The determination of the detonation pressure is presented in Figure 9 for an OWC sample. Thereby, p-u-Hugoniot (derived from conservation laws) of the flyer is calculated from the material properties of the aluminum. The anchor point of the right-going Hugoniot is defined at zero pressure at zero particle velocity due to the resting condition prior to the shock. The corresponding rarefaction wave (left-going Hugoniot, not drawn) anchors at zero pressure, and the measured free surface velocity from PDV, which equals twice the particle velocity. A correction is required to determine the particle velocity at the interface from the measured free surface velocity due to losses of the shock wave passing the flyer. This correction is done similarly to the extrapolation method proposed by Lorenz et al. [10], which requires a high spatial resolution in the PDV spectrogram using a high sample rate of 40 GS/s. This velocity correction introduces the main uncertainty of this method for determining the detonation

TABLE 3 | Results of the investigations of granulates and pellets with X-ray diffraction techniques.

XRD technique	Rietveld analysis		Sigmoidal fit of the width distribution		
Sample	**Density** [g/cm³]	**Size**[a] [nm]	x_0[b] [°2θ]	**p**[c] [–]	**CoD**[d] [–]
Granulates					
HWC	—	—	0.0650 (3)	3.00(5)	0.993
OWC	—	—	0.0866 (8)	2.20(4)	0.991
PHX 151	—	—	0.0771 (7)	2.36(6)	0.981
PHX 153	—	—	0.0634 (5)	2.93(8)	0.968
Pellets					
HWC	1.777	88.9	0.1161 (3)	3.63(4)	0.997
OWC	1.894	69.1	0.1675 (5)	3.84(8)	0.994
PHX 151	1.895	59.9	0.1761 (12)	3.42(9)	0.988
PHX 153	1.948	110.8	0.1138 (7)	3.27(6)	0.996

[a]Mean volume weighted mean crystallite size, calculated from integral breaths;
[b]Center and
[c]power of peak the width distributions;
[d]Coefficient of determination; Standard deviations in brackets refer to the last digit.

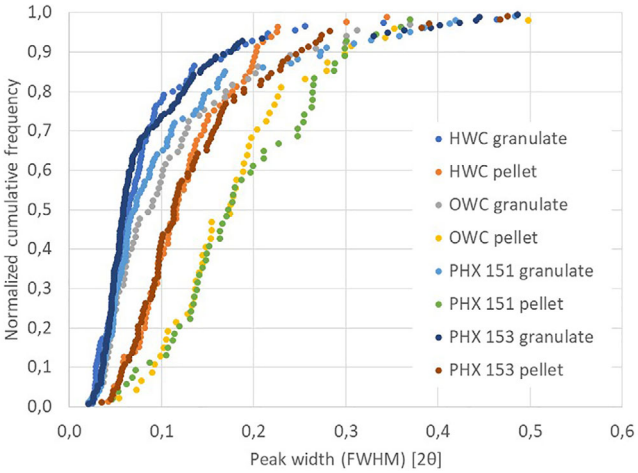

FIGURE 6 | Comparison of cumulative diffraction peak width distributions of granulates and pellets.

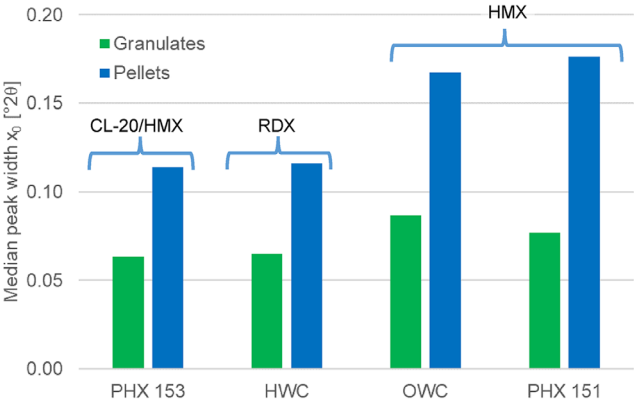

FIGURE 7 | Median peak widths of granulates and pellets. Higher values correlate to smaller crystallite domains (i.e., pronounced crystal damage). Standard deviations of sigmoidal fits were below 0.0015.

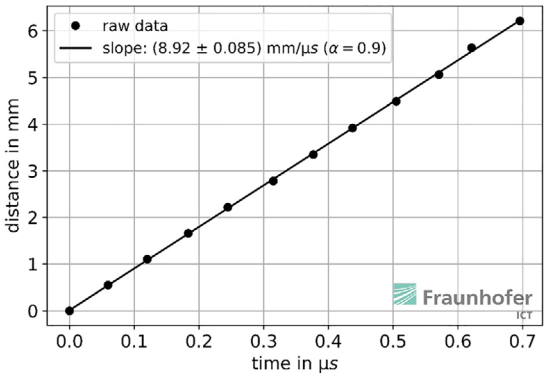

FIGURE 8 | Example of a pin position (probe distance) vs circuit time correlation of a detonation front running through a PHX 153 pellet.

pressure. However, this correction is done identically to all tests applied within this investigation. The uncertainty is therefore representative of the test setup and should be negligible while comparing the results of this study.

This allows us to determine the pressure at the interface state (between the explosive and flyer). The left-going Hugoniot is defined by the general Cooper equation of state (Cooper-EOS) [16]. This Hugoniot anchors at the common interface state (between flyer and explosive). Finally, the Rayleigh line (defined by the measured detonation velocity and the known initial density), which ensures mass- and momentum conservation, defines the Chapman-Jouguet (CJ) point at the intersection of the Cooper-EOS. This leads to the detonation pressure. An alternative solution is derived by using the acoustic approximation [17] by linearizing an EOS based on the slope of the Rayleigh line. However, both solutions (Cooper-EOS and acoustic approximation) have been found to be very similar, which also applies to previous findings. Therefore, a visual distinction between both CJ-points

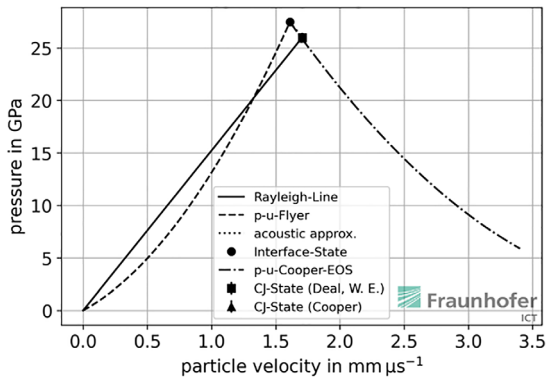

FIGURE 9 | Visualization of the impedance matching in the case of an oktogen/wax/graphite formulation (OWC) sample.

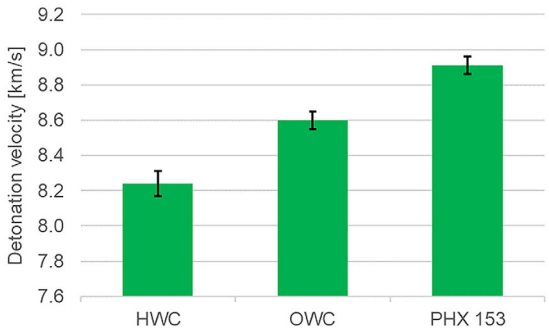

FIGURE 10 | Comparison of detonation velocities of the explosive formulations hexogen/wax/graphite formulation (HWC), oktogen/wax/graphite formulation (OWC), and PHX 153 with standard errors.

in Figure 9 is not possible, and only the CJ-conditions resulting from acoustic approximation are shown in the following.

The errors provided by both methods result from the statistical evaluation of repeated trials. As the number of trials was limited due to the high experimental effort and the limited number of energetic samples, the Student's t-distribution was applied to the standard errors to account for the sample size. Figure 10 compares the mean detonation velocities and standard errors of the explosives HWC, OWC, and PHX 153.

The evaluation yielded detonation velocities of 8.24 ± 0.07 km/s for HWC, 8.6 ± 0.05 km/s for OWC, and 8.91 ± 0.05 km/s for the cocrystal-based PHX 153, that is, the application of the cocrystal increased the detonation velocity by 0.31 km/s (3.6%) and 0.67 km/s (8.1%) compared to the HMX- and RDX-based formulations OWC and HXC, respectively. As the differences are greater than the standard errors, the results are considered significant. Due to the small setup, there might be a small systematic error due to the short run distance and the small charge diameter (in terms of the critical diameter), which applies to the absolute values. In 2022, slightly higher reference values of 8.4 km/s (HWC) and 8.8 km/s (OWC) were measured for samples with 21 mm diameter and 60 mm length. However, due to the identical sample geometries and experimental setup within this investigation, only the differences with respect to the error bands are relevant for the interpretation.

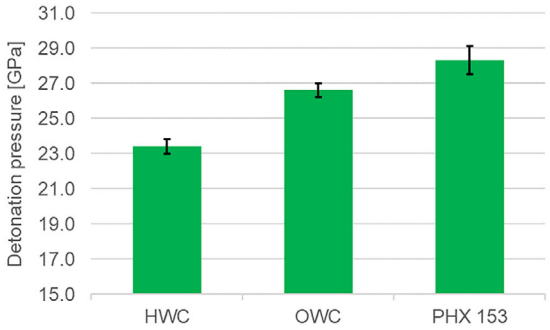

FIGURE 11 | Comparison of detonation pressures P_{CJ} of the explosive formulations hexogen/wax/graphite formulation (HWC), oktogen/wax/graphite formulation (OWC), and PHX 153 with standard errors.

TABLE 4 | Detonation velocities and pressures with standard error (90% confidence interval) compared to reference data measured with 21 mm charges in 2022.

	This work (10 mm)	Reference 2022 (21 mm)
Detonation velocity [km/s]		
HWC	8.24 ± 0.07	8.4 ± 0.17
OWC	8.6 ± 0.05	8.8 ± 0.08
PHX 153	8.91 ± 0.05	—
Detonation pressure [GPa]		
HWC	23.4 ± 0.4	25.8 ± 0.08
OWC	26.6 ± 0.4	28.6 ± 1.20
PHX 153	28.3 ± 0.8	—

A similar ranking was found for the detonation pressures, with 23.4 ± 0.4 GPa for HWC, 26.6 ± 0.4 GPa for OWC, and 28.3 ± 0.8 GPa for PHX 153 (Figure 11), that is, detonation pressure was increased by 1.7 GPa (6.4%) and 4.9 GPa (20.9%) in the cocrystal-based PHX 153 compared to OWC and HWC, respectively. Again, the differences are greater than the standard errors and thus significant, and the currently measured detonation pressures of HWC and OWC were smaller by about 10% and 7% than the reference values measured in 2022 (Table 4). The results suggest that with the current charge geometry, the absolute detonation pressures are not yet ideal, but a reasonable relative comparison of the explosive formulations was achieved.

4 | Conclusions

The investigation proved the feasibility of the production of PBX granulates and pressed pellets with CL-20/HMX cocrystal on a paraffin basis. Moreover, pellets of the cocrystal-based PHX 153 and reference PBX were produced (PHX 151) or commercially obtained (HWC and OWC) and characterized by means of XRD and small-scale detonation test. The CL-20/HMX cocrystal/wax/graphite formulation PHX 153 was less sensitive against frictions and impact than the commercial OWC, particularly the limiting friction force increased to 324 N compared to 160 N for OWC, and thus nearly reached the limit of 350 N

for low sensitive materials. Comparing the sensitivities of the explosive/wax/graphite granulates to HMX/hydroxyl-terminated polybutadiene-based PBX formulations with partial replacement of HMX by CL-20/HMX-cocrystal (of earlier investigations) revealed a significantly higher impact sensitivity (6 Nm compared to 15 Nm), but the same friction sensitivities (324 N). Hence, application of the CL-20/HMX cocrystal may reduce friction sensitivities to approximately low-sensitivity formulations compared to a CL-20 formulation. This might be of particular interest, as incidents with CL-20 occurred in cases where friction was supposed to drive an initiation. However, with the high impact sensitivity of the co-crystal (1.5–4.5 Nm), further approaches shall aim to produce reduced sensitivity variants with high purity, low defect concentration, and a smooth spherical particle shape, and moreover, the application of soft mixing processes would be recommended, for example, acoustic mixing. A further approach may include particle coating of the cocrystal with an insensitive layer.

The non-destructive microstructure investigations of the cocrystallized raw product identified the reported crystal structure with the absence of crystalline impurities or unconverted precursors. The granulation and pressing of the explosives did not induce any phase transitions or disintegration into precursors. Furthermore, different mechanical strengths of the explosive crystals were detected in terms of the response after loading and susceptibility to failure. The peak broadening of the crystals indicated a higher mechanical stability of embedded RDX crystals in HWC and CL-20/HMX cocrystals in PHX 153 compared to HMX crystals in OWC and PHX 151. The observations are in coincidence with findings reported in literature, where HMX is considered to be brittle compared to other secondary explosives and, moreover, deformation twinning occurs in HMX at lower mechanical loading, preceding fracture [18–20]. Both deformation twinning and fracture of embedded crystals will also impact the mechanical strengths of the related compositions, OWC and PHX 151. The small-scale detonation tests yielded 8.91 km/s and 28.3 GPa detonation velocity and pressure of the cocrystal-based PHX 153, and thus significant increases of 0.31 km/s (3.6%) and 1.7 GPa (6.4%) compared to the HMX-based OWC.

So far, the CL-20/HMX cocrystal proved to be a promising candidate to increase the detonation performance, e.g., of pressed explosive formulations with higher mechanical stability of the embedded crystals and improved friction sensitivity compared to CL-20, but the high impact sensitivity of the raw product still must be considered. Further investigations shall verify these findings and include medium- or large-scale performance tests.

Acknowledgments

Open access funding enabled and organized by Projekt DEAL.

Data Availability Statement

The authors have nothing to report.

References

1. O. Bolton and A. J. Matzger, "Improved Stability and Smart-Material Functionality Realized in an Energetic Cocrystal," *Angewandte Chemie* 123 (2011): 9122–9125.

2. O. Bolton, L. R. Simke, P. F. Pagoria, and A. J. Matzger, "High Power Explosive With Good Sensitivity: A 2:1 Cocrystal of CL-20:HMX," *Crystal Growth & Design* 1, no. 9 (2012): 4311–4314, 10.1021/cg3010882.

3. H. Gao, W. Jiang, J. Liu, et al., "Synthesis and Characterization of a New Co-Crystal Explosive With High Energy and Good Sensitivity," *Journal of Energetic Materials* 35, no. 4 (2017): 490–498.

4. D. Herrmannsdörfer, P. Gerber, T. Heintz, M. J. Herrmann, and T. M. Klapötke, "Investigation of Crystallisation Conditions to Produce CL-20/HMX Cocrystal for Polymer-bonded Explosives," *Propellants, Explosives, Pyrotechnics* 44 (2019): 668–678, 10.1002/prep.201800332.

5. D. Herrmannsdörfer, M. Herrmann, T. Heintz, and P. Gerber, in *Proceedings of the 50th International Annual Conference of the Fraunhofer ICT*, June 25–28, 2019. 36 (2019): 1–2.

6. D. Herrmannsdörfer and T. M. Klapötke, "High-Precision Density Measurements of Energetic Materials for Quality Assessment," *Propellants, Explosives, Pyrotechnics* 46 (2021): 413–427, 10.1002/prep.202000272.

7. D. Herrmannsdörfer and T. M. Klapötke, "Quality Assessment of the CL-20/HMX Cocrystal Utilising Digital Image Processing," *Propellants, Explosives, Pyrotechnics* 46 (2021): 522–529.

8. M. Herrmann and P. Gerber, in *Proceedings of the 52nd International Annual Conference of the Fraunhofer ICT*, June 27–30, 2023, Karlsruhe, Germany. 48 (2023): 1–11.

9. P/O/Weber Laborpresstechnik, https://www.p-o-weber.de/.

10. K. T. Lorenz, E. L. Lee, and R. Chambers, "A Simple and Rapid Evaluation of Explosive Performance—The Disc Acceleration Experiment," *Propellants, Explosives, Pyrotechnics* 40 (2015): 95–108.

11. T. M. Baust, "Downscaling the Methodology for Determining Detonation Velocities Applied to Small Sample Quantities of Explosives," *Fraunhofer-Gesellschaft* (2022), 10.24406/publica-136.

12. T. Baust, "Energetic Materials—Exploring and Understanding," in *Proceedings of the 51st International Annual Conference of the Fraunhofer ICT* 64 (2022): 1–7.

13. R. A. Young, *The Rietveld Method* (Oxford University Press, 1995).

14. Bruker, *TOPAS-32 V6, User Manual*, (Bruker AXS GmbH, 2017).

15. International Centre for Diffraction Data (ICDD), Powder Diffraction Database (PDF-2), 2025, https://www.icdd.com/.

16. P. Cooper, *Explosives Engineering* (Wiley-VCH, 1996).

17. W. E. Deal Jr, "Detonation Pressures in Solid Explosives," in *2nd Symposium on Detonation* (Office of Naval Research, 1955): 209–224.

18. H. G. Gallagher, J. C. Miller, D. B. Sheen, J. N. Sherwood, and R. M. Vrcelj, "Mechanical properties of β-HMX," *Chemistry Central Journal* 9 (2015): 22.

19. S. J. P. Palmer and J. E. Field, "The Deformation and Fracture of β-HMX," in *Proceedings of the Royal Society of London A* 383 (1982): 399–407.

20. R. Armstrong, H. Ammon, Z. Du, et al., "Energetic Crystal-Lattice-Dependent Responses," in *MRS Online Proceedings Library* 296 (1992): 227–232.

doi:10.24406/publica-6150